Research Article

Open Access Journal of Applied Science and Technology

# Lithium-Sulphur Batteries – Their Equivalent Circuit Model and How Electrochemical Conductivity Impacts Resistivity and Capacity Fading

**Ahmad Ali Khan* and Mohamed Zohdy**

*Department of Electrical and Computer Engineering, Oakland University, Rochester, MI*

***Corresponding Author**
Ahmad Ali Khan, Department of Electrical and Computer Engineering, Oakland University, Rochester, MI.

**Submitted:** 2023, May 01; **Accepted:** 2023, May 29; **Published:** 2023, Jun 06

**Citation:** Khan, A. A., Zohdy, M. (2023). Lithium-Sulphur Batteries – Their Equivalent Circuit Model and How Electrochemical Conductivity Impacts Resistivity and Capacity Fading. *OA J Applied Sci Technol,* 1(1), 01-09.

## Abstract

*Electrochemical impedance spectroscopy (EIS) was used to investigate the Lithium Sulfur battery's electrochemical dynamics. An equivalent circuit model was created using temperature and discharge depth data from EIS spectra. The mechanism of Lithium Sulfur batteries' capacity depletion was then studied by tracking the change in impedance during cycling. According to the findings, the charge-transfer mechanism is responsible for the EIS spectrum's semicircle at intermediate frequencies, whereas the high-frequency semicircle is linked to the interfacial electrical resistance. Additionally, the key significant contributor to the capacity fading of Lithium Sulfur batteries' is the charge-transfer impedance, whereas electrolyte resistance and interphase contact resistance also fluctuate with cycle number, albeit in different ways.*

**Keywords:** Lithium/Sulphur Battery, Electrochemical Impedance Spectroscopy, Conductivity, Impedance, Charge Transfer

## 1. Introduction

The Lithium Sulphur (LiS) batteries, with their high-power density and high estimated specific capacitance (1675 mAhg1), are promising power storage technologies for the next generation of lithium-ion batteries (2600 Whkg1). Sulphur has proved to be an ideal active cathode material due to its abundance in nature and decreased effect on the environment [1,2]. Polysulfides are soluble as input materials due to the insulating nature of sulphur. However, insoluble agglomerates of irreversible discharge products pose serious challenges to the commercialization of LiS batteries due to their impact on material utilization and battery life (Li2S2 and Li2S). In order to develop lasting answers to these problems, we must have a firm grasp of the electrolytic method and the aging process of LiS devices [3].

As one of the most effective electroanalytical instruments, electrochemical impedance spectroscopy (EIS) has been used extensively for the investigation of kinetics in several electrochemical systems. Applying a circuit model to aid in the interpretation of the data is often necessary to identify the portions of the EIS spectrum that correspond to respective physical or chemical processes and to calculate kinetic parameters. Recent research on the electrochemical characteristics of LiS batteries has made use of EIS [4,5]. An EIS spectrum is composed of three components: two semicircles with depressions, and a slanted line. The HF concentric circle has been attributed to charge-transfer resistance in certain reports, while the MF semicircle has been attributed to a sample directly composed of Li2S and Li2S2 [6]. However, the concentric circle at HF is associated with solid film resistance, whereas the circumferential circle at MF is associated with charge-transfer impedance in the models of other authors [7]. Therefore, "overall" EIS models for the LiS battery must be re-evaluated.

Much of the prior EIS research on LiS batteries has been conducted to understand the electrochemical mechanism and dynamics during a single cycle. Polysulfide effect on charge state as an impedance function was investigated. The results imply that electrolyte conductivity significantly affects the speeds of electrochemical reactions [8]. The form of the EIS spectrum was investigated as they measured the sulphur cathode at several voltages throughout a given cycle [9]. When the Sulphur multi-walled… was initially developed, they investigated the influence of discharge depth on the cathode by studying the EIS fluctuation [10]. First-cycle sulfurized polyacrylonitrile composite cathode was investigated by Wang et al. using EIS [9]. Furthermore, they produced a suflur-carborn spherical composite, and measured EIS for the composite cathode after 1, 20, 50, and 100 cycles [11]. Zhange et al. concluded the composite with improved cyclability exhibited less extreme changes in impedance as a consequence of cycling. To the best of our knowledge, however, the EIS technique has not been systematically used in the study of the capacity fading phenomenon of LiS batteries.

In the current study, we use analyses of EIS spectra at different temperatures and discharge depths to propose an Equivalent Circuit Model for the LiS battery. Following this, we track the LiS battery's impedance fluctuation as a function of cycle number to learn more about the electrochemical conductivity and capacity fading process. The initial discharge procedure and the kinetic

parameters during progressive cycling are also described.

## 2. Research Methodology

N-methyl-2-pyrrolidinone (NMP) solvent was used to create a slurry consisting of 60% sublimed Sulphur, 30% carbon black, and 10% polyvinylidene fluoride (PVDF). After spreading the slurry over aluminum foil (20 m), it was dried at 60 C in a vacuum for 24 hours. The electrodes took the shape of a cylindrical coin with a diameter of 10mm, and the sulphur diameter, and the sulphur loading carried a mass of 1 mg/cm$^2$.

An argon-filled glove box (Universal 2440/750) with oxygen and water levels below 1 ppm was used to assemble CR2025 coin cells. The electrolyte was a mixture of 1,3-dioxolane (DOL) and 1,2-dimethoxyethane (DME) (1:1, v/v) (Acros Organics) containing 1.5M bis(trifluoro-methane) sulfonamide lithium salt (LiTFSI, Sigma Aldrich). The counter electrode was made from lithium metal foil, while the separator was made from Celgard 2400. At 25 degrees C, a LAND CT2001A charge-discharge system was used for galvanostatic charge/discharge testing at a constant current density of 168 mA g1 (0.1 C) throughout a potential range of 1.5 to 3.0 V. The PARSTAT 2273 electrochemical measuring equipment was used to take the EIS readings (PerkinElmer Instrument USA). Cell impedance spectra were obtained with a perturbation amplitude of 5 mV in the frequency range of 100 kHz to 10 MHz. The EIS testing was conducted in a high-low temperature test chamber (GDH-2005C) which maintained a constant temperature. ZView was used to make a fitting of the collected EIS data.

## 3. Results and Discussion

**3.1 Impedance Variations and Temperature Effects** - Because different resistance properties are temperature-dependent, LiS cell EIS tests were carried out at 0, 10, 25, and 40C [12,13]. The batteries were measured when fully charged following 20 cycles with an open-circuit voltage of 2.33 V. Due to the cells' apparent self-discharge propensity, the open-circuit voltage decreased to 2.18 volts when the temperature was increased to 40 degrees C, which is much lower when compared to that which was recorded in the previous four levels. Nyquist diagrams for an LiS battery are shown in Figure 1 across a range of temperatures. It can be seen in the Nyquist plots that the high-frequency (HF) area (100 kHz-1 kHz) is represented by two semicircles that partially overlap, while the low-frequency (LF) area is represented by a straight, sloping line (1 Hz-10 MHz). It is clearly shown that as the temperature decreases, the size of the MF semicircle increases substantially.

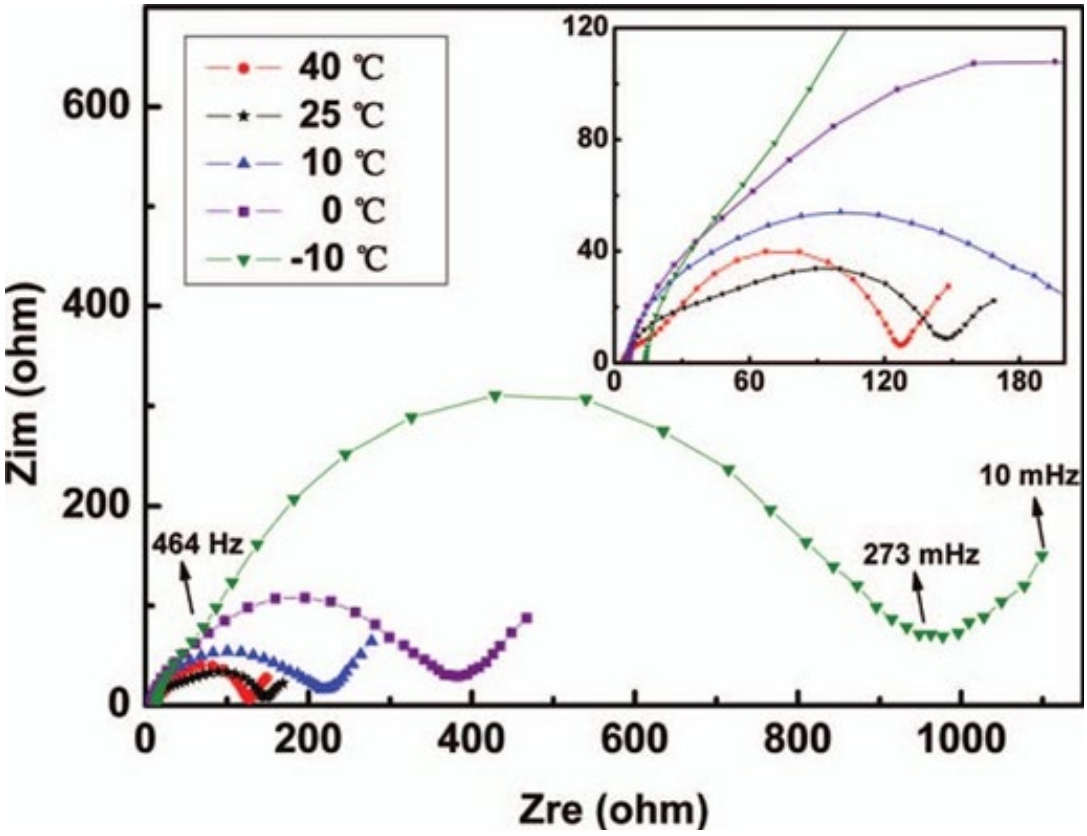


**Figure 1:** LiS Nyquist Plot

Zview program examined the Nyquist plots to better comprehend the variation of impedance characteristics. Here, we suggest a simpler circuit for the EIS spectra depending on the characteristics of the Nyquist plot, as shown in Figure 2. This R1 represents the electrolyte's resistance [9].

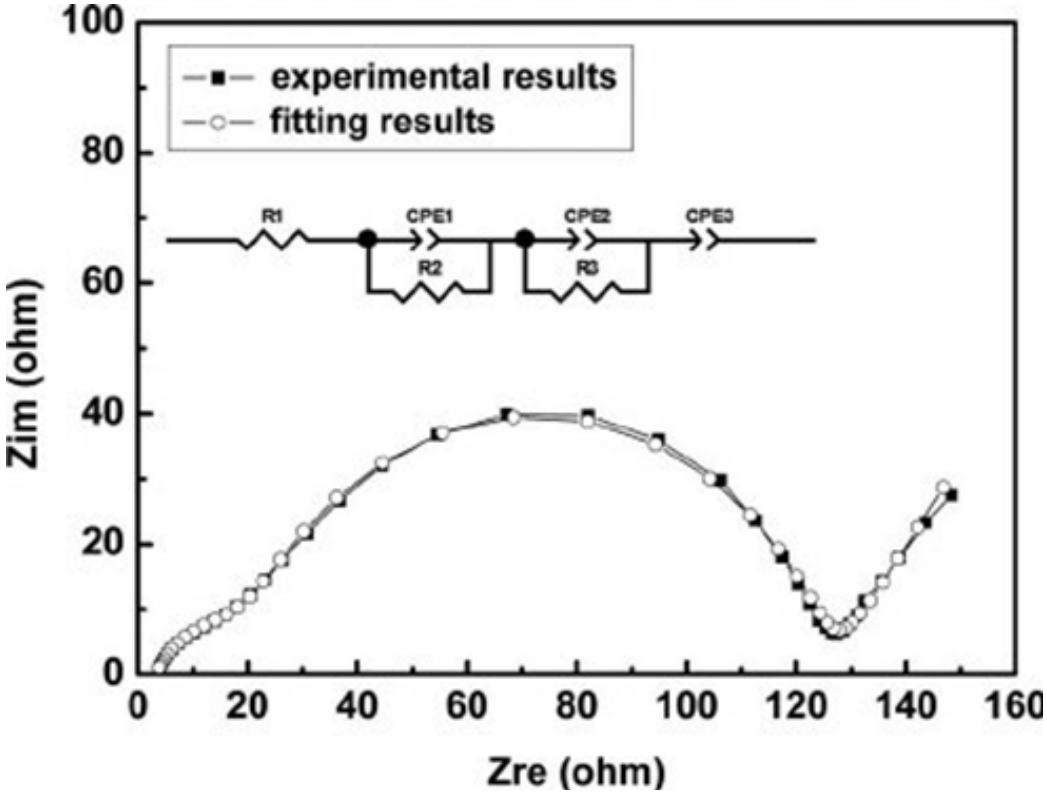


**Figure 2:** Equivalent Circuit Analysis of an LiS Nyquist Plot

The Figure 1 spectra fitted R1, R2, and R3 values are shown as a function of temperature. Studies on lithium batteries have revealed (as shown in Figure 3) that the conductivities of the electrolytes decrease with decreasing temperature, which leads to an increase in R1. In contrast, R3 increases significantly from 106 - 854 with gradual decrease in temperature from 40 °C and 10 °C [13,14]. This reaction demonstrates that heat-induced charge transfer occurs along the half-circle at MF [12,15]. R2 is unaffected by temperatures between 10- 25°C. Although it was predicted that a temperature-dependent shift in R2 would be shown if the semicircle at HF was linked to the diffusion of ions between the cathode's solid covering and the lithium electrode, our experiments indicated otherwise. As is demonstrated by the aforementioned research, the semicircle in HF may have more than a passing acquaintance with the basic ionic conduction mechanism through a coating material on the electrode. Consequently, the relationship between impedance and DOD was investigated.

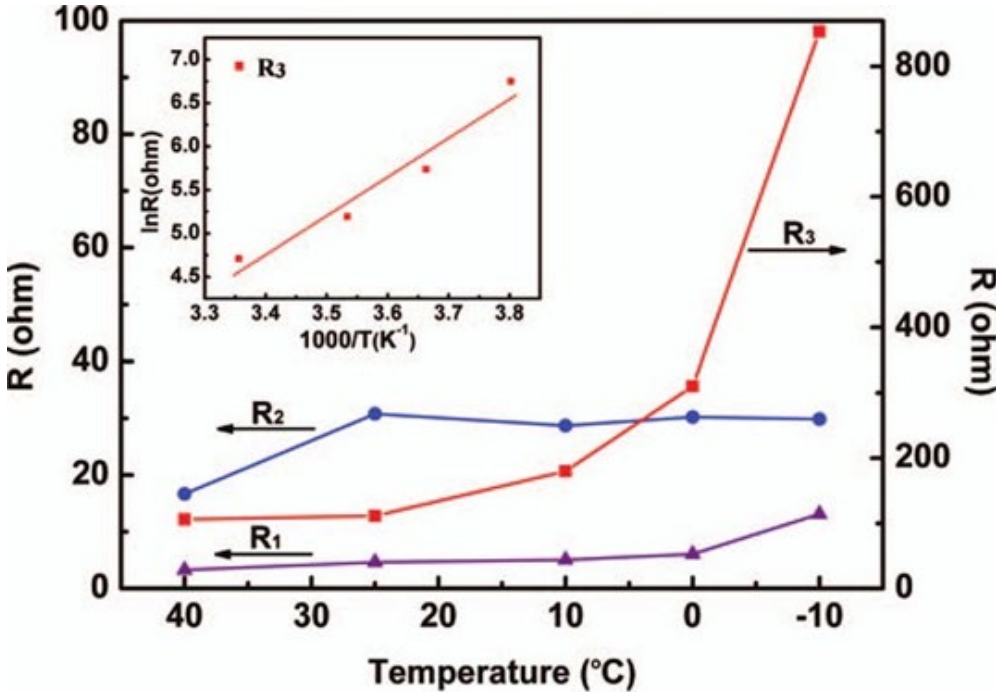


**Figure 3:** Resistance Parameters Temperature Dependence of LiS

### 3.2 Impedance Variation and Discharge Depth

The first-cycle discharge curve of an ordinary LiS cell is shown in Figure 4. There are two possible plateaus in the discharge curve. There is a lower plateau associated with the conversion of solubility lithium polysulfides into impassable disassemblers (Li2S2 and Li2S). And a higher plateau is associated with the conversion of insulated Sulphur into liquid high-order lithium polysulfides [1].

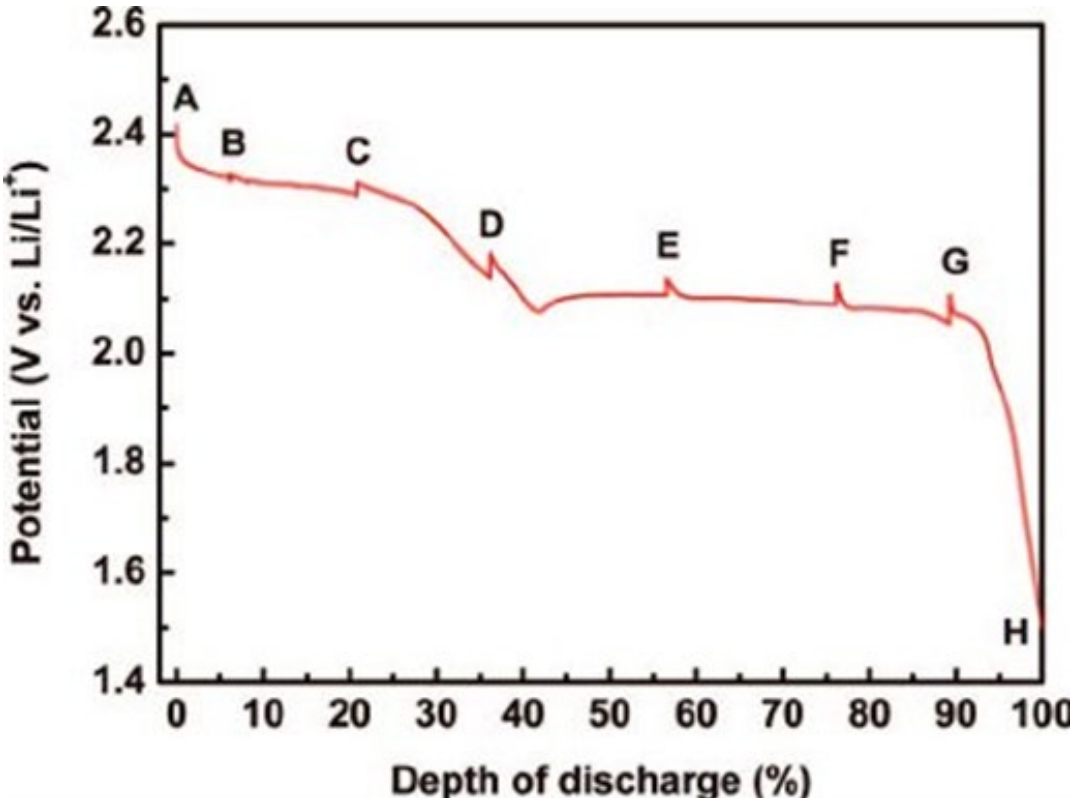


**Figure 4:** Lithium/Sulfur Discharge Curve

Nevertheless, in some studies of lithium batteries, the HF concentric circle has been interpreted as interfacial electrical resistance in the electrode's core [16,17]. Intake of Sulfur facilitates enhanced electric interaction between particles in the interphase, the HF semicircle is reduced, and insulating materials are created. Particles with reduction products on their surfaces may have a higher interphase contact resistance and a somewhat larger HF semicircle. The anode resistance in a polysulfide-containing electrolyte is negligible and lacks significant contribution to the evolution of HF semicircles and is therefore disregarded. In light of the findings above, the equivalent circuit model shown in Figure 5 is presented as a potential solution. Potential illustrations of the physical/chemical process of the Sulphur electrode are shown. When Sulphur particles are present in the cathode as shown in Figure 5a, the generation of solid products is seen in 5b, indicating complete Sulphur reduction. The suggested circuit model includes electrolyte resistance (denoted by Re) as one of its parameters.

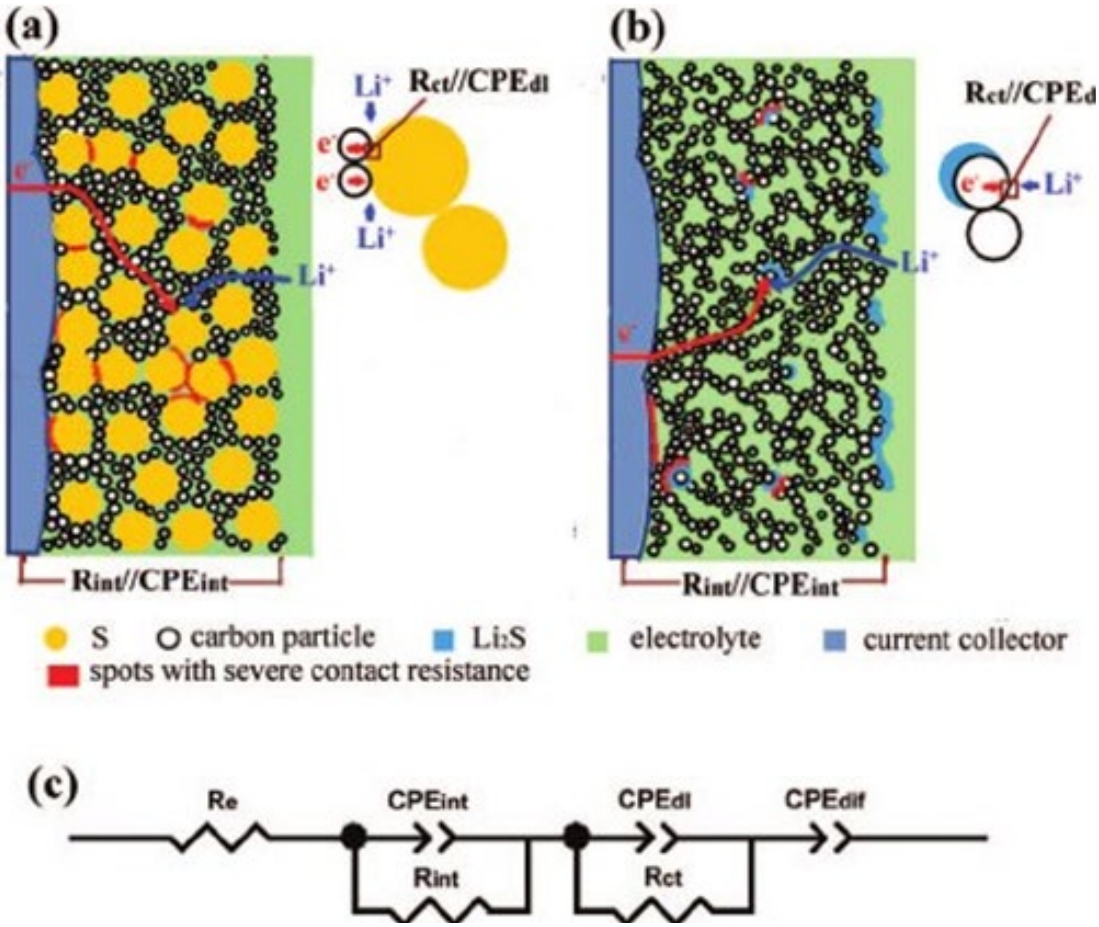


**Figure 5:** Physical/Chemical Processes Involved in the Sulfur Cathode: (a) Sulfur particles exist. (b) Sulfur is reduced. (c) The proposed equivalent circuit for lithium-sulfur cells.

The electrons propagation from the conductive substrate to the reactive species is modeled by the Sulphur electrode's bulk capacitance, CPEint, and the interphase contact resistance, Rint. The rate of charge transfer between the conducting substance and the electrolyte at the interface is represented by the ratio of the charge-transfer resistance (Rct) to the charge capacitance (CPEdl). The diffusion impedance, denoted by the symbol CPEdif, is likely a proxy for the diffusion of Li-ions. The Nyquist plots were studied using the equivalent circuit shown in Figure 1 to have a better understanding of the primary events happening during the first discharge phase [6].

Figure 6 is a scatter plot showing the Re, Rint, and Rct vs DOD. From point A (0 percent DOD) in Figure 7a down to point D (36 percent DOD) and back down to the end of discharge, Re increases. Other sources have observed similar findings [5,7]. As the discharge continues, Sulphur converts to soluble polysulfides, increasing the electrolyte's viscosity and, in turn, its resistance. After the polysulfides are broken down into insoluble Li2S and Li2S2, the viscosity of the electrolyte decreases, and the electrolyte becomes less resistant to current.

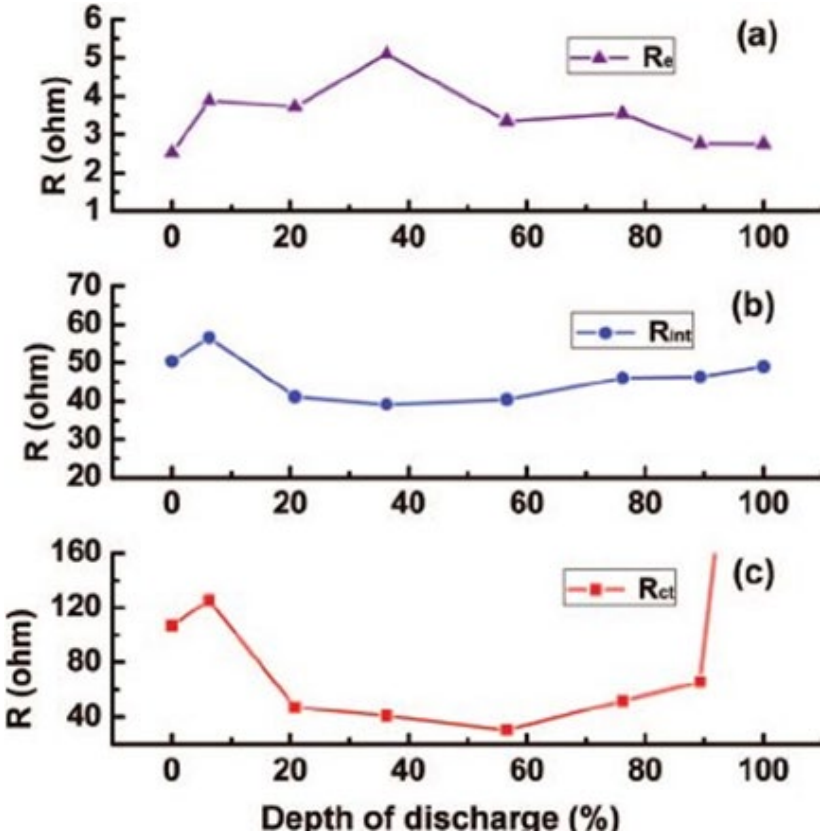


**Figure 6:** LiS Resistive Plots

Rint values at various discharge depths are shown in Figure 6b. Early in the discharge process, the Rint level rises (point B). The movement of particles during an electrochemical response may be responsible for this phenomenon. Starting at point B (6% DOD), Rint rapidly declines to point C (21% DOD). After some early volatility, the Rint begins a slow and steady ascent. The removal of insulator Sulphur may be responsible for the noticeable decrease in Rint, while the subsequent increase in Rint seems likely linked to the production of non - conducting disassemblers.

Figure 6c shows the shift in Rct concerning DOD. Similar to the behavior of Rint, Rct's value begins to increase initially during discharge, then begins decreasing and reaches a value of 30.6. A peak Rct of 65.7 was attained at timestep G (89 percent DOD). The large decrease in Rct from points B to C is related to increased electrochemical permeability due to Sulphur absorption, whereas the rise in Rct from points A to B may be attributed to the creation and buildup of insulated Li2S and Li2S2 and considerably less solvent polysulfides. Point H on the Nyquist diagram indicates that the discharge mechanism has concluded, displayed an arc in lieu of the MF semicircle, and the LF area exhibits the hallmarks of a large arc. This is because a Sulphur electrode surface completely coated with insulating precipitations functions as a blocking barrier, preventing the charge from passing through [6]. The findings point to a tight relationship between the electrical conductivity of the Sulphur cathode and the kinetics of the transfer process.

### 3.3 Impedance Variations and Cycle Number

Capacity fading is a major issue that arises from extended cycling, which is common in LiS batteries. An LiS cell's discharge and charge curves are shown in Figure 7. The discharge capacity decreases dramatically in the first few cycles, stabilizes after about 13 cycles, and gradually fades thereafter. Cyclicity was also seen in several experiments of Sulphur cathodes [18]. It has been found that polysulfide solubility is a factor in capacity degradation [11,1]. The charge process will take longer to complete, fewer redox reactions will be used during the discharge, and the capacity will fade due to the polysulfide shuttle phenomenon. The capacity degradation is further influenced by the precipitation of persistent and electrochemically inaccessible crystallites (Li2S and Li2S2) on the cathode [11]. Although several studies do not recognize the shuttle phenomena, their cyclability is not diminished thereof. The capacity fading process of the Sulphur cathode was studied by measuring EIS and observing the impedance change over time while the cycled battery was charged and discharged [19,20]. All tests were performed on cells that were charged to 3.0 V at 0.1 C and held at that voltage for 1 h.

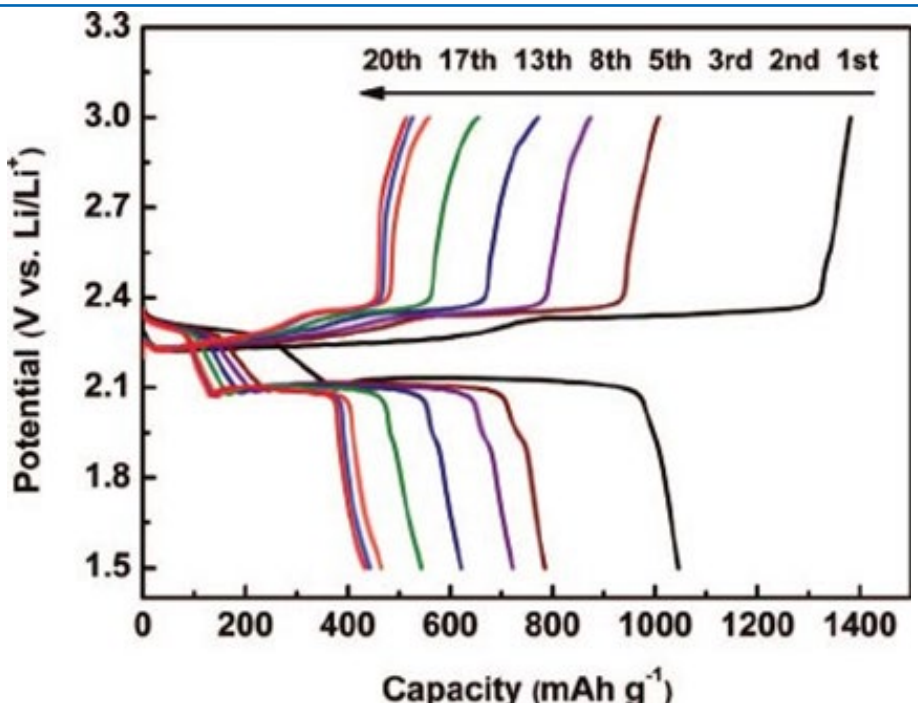


**Figure 7:** LiS Charging and Discharging Characteristics

Nyquist plots of the Sulphur electrode are shown in Figure 8 for many different cycles. During the first eight cycles, the MF semicircle's magnitude grows dramatically, indicating a tight link between impedance and capacity fading. For this purpose, the circuit design shown in Figure 5 was used to fit Nyquist plots.

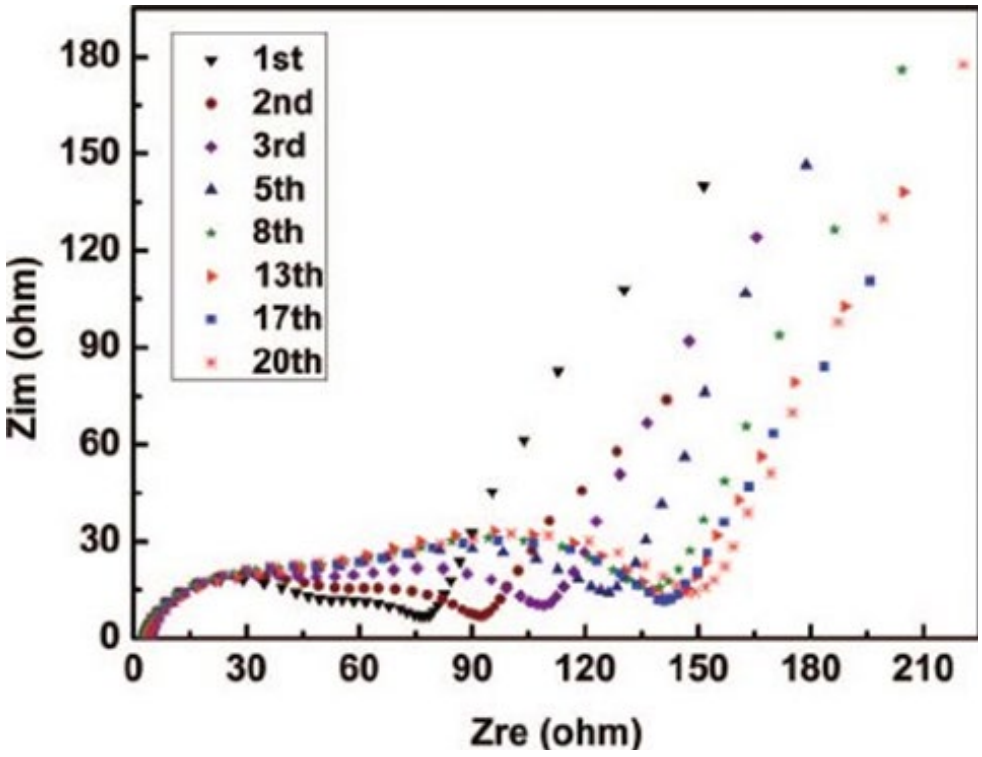


**Figure 8:** LiS Cell Series Charge Cycles

A scatter plot of Re, Rint, and Rct vs cycle number is shown in Figure 9. Different patterns of change in Re, Rint, and Rct may be seen as the cycle number increases. After an initial surge over the first eight cycles, the Rct settles into a more gradual ascent The Re maintains consistent values throughout the duration of all cycles. The Rint shows some variance in its outcomes between the third and thirteenth cycles, then experiences a gradual increase. One possible explanation for this is that as the cathode undergoes several cycles, internal cracks begin to occur [21]. Analyzing the relationship between the discharge coefficient and the changes in three resistivity values (Re, Rint, and Rct) led us to the conclusion that Rct is a crucial factor in the degradation of LiS battery performance as shown in Figure.7.

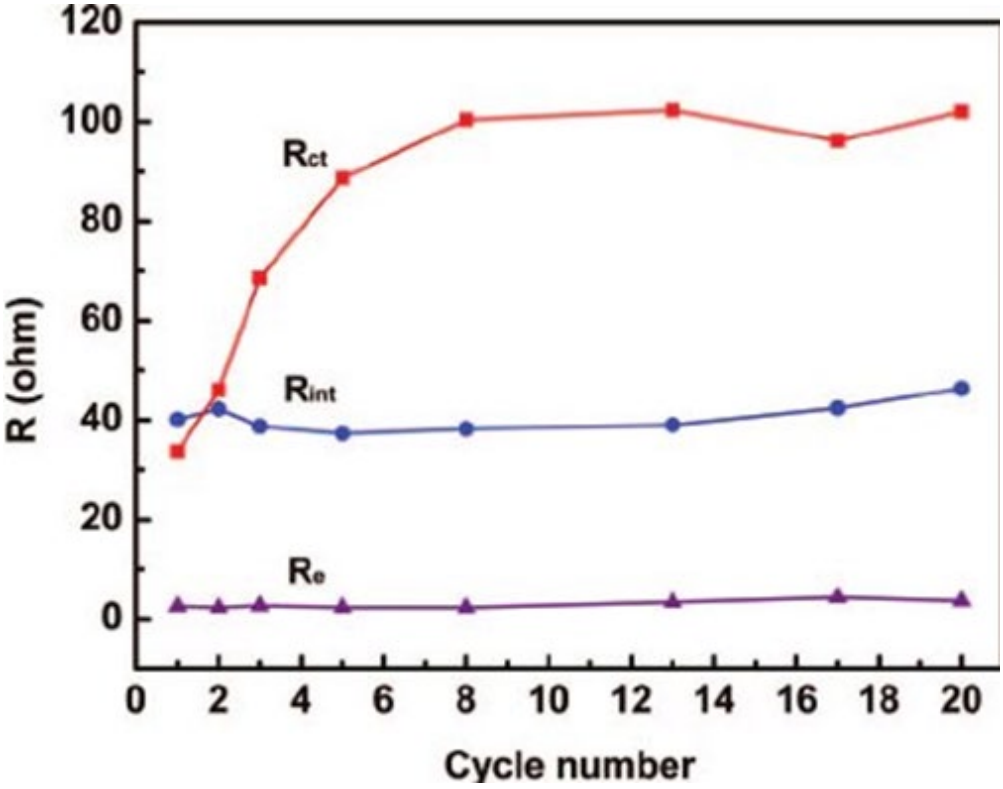


**Figure 9:** LiS Electrolytic and Conductive Resistance as a Function of Cycle Number

A significant component that contributes to the remarkable rise in Rct is the deterioration of the cathode's surface. Throughout the charging process, insulated discharge agents (Li2S, Li2S2) are re-oxidized to solubility polysulfides. However, even in the fully charged state, only a limited number of these polysulfides are present. As a result, the cathode's surface develops insulated agglomerates of residual Li2S and Li2S2 as the number of cycles rises. After studying the surface conductance of a Sulphur electrode, it can be stated that as cycling progressed, the electrode surfaces became less conductive [22]. The research further confirmed the study in discussion. It is also well-established that the interface between the conducting additives and the electrolytes is the site of charge-transfer operations. Therefore, the increased Rct could be associated with the accumulation of nanocrystals, which also reduce the high conductivity region on the surface of the cathode and hinders the mobility of ions into the interior of the cathode, resulting in sluggish transference reactions kinetics and capacity fading. This is because cumulative agglomerates reduce the area of the cathode surface that is electrically conductive.

As previously stated, the fissures that manifest themselves inside the Sulphur cathode after several cycles may be associated with the subsequent smooth rise in Rct. The cathode substance that is exposed inside the fissures may still be reached electrochemically, even if the surface conductance is minimal. Further, the fissures allow for efficient interaction between solutions species and conducting carbon-based material. The findings presented above provide evidence that Rct has a direct connection to the surface characteristics of the Sulphur cathode.

## 4. Conclusion

The fluctuations in impedance that occur as a temperature function and discharge state suggest an equivalent circuit model that can be applied to an LiS battery. The capacity fading process is then investigated using a series of EIS measurements that are carried out at a variety of cycle numbers. The findings suggest that the transfer of charge impedance and its comparable capacitance determine the semicircle at a moderate frequency; whereas at a high frequency, the semicircle may be related to the interfacial electrical resistance. In addition to the conductance of the Sulphur cathode and the cathode surface properties, the increase in charge-transfer impedance plays a crucial role in the deterioration of an LiS battery's capacity. This is due to the cathode's surface characteristics and the conductivity of Sulphur. As a result, to lessen the charge-transfer impedance of LiS batteries and enhance their cycle stability, it is crucial to develop effective cathode materials that help to prevent catastrophic agglomerates on the cathode surface.

## References

1. Bruce, P. G., Freunberger, S. A., Hardwick, L. J., & Tarascon, J. M. (2012). Li–O2 and Li–S batteries with high energy storage. Nature materials, 11(1), 19-29.
2. Ji, X., & Nazar, L. F. (2010). Advances in Li–S batteries. Journal of Materials Chemistry, 20(44), 9821-9826.
3. Cheon, S. E., Choi, S. S., Han, J. S., Choi, Y. S., Jung, B. H., & Lim, H. S. (2004). Capacity fading mechanisms on cycling a high-capacity secondary sulfur cathode. Journal of the Electrochemical Society, 151(12), A2067.
4. Li, Y., Xing, B., Ma, J., Peng, S., Li, Y., Zhou, K., ... & Yang, S. (2022). One-step synthesis of nano-S/C@ PANI composites for lithium-sulfur batteries with high rate and

long lifespan. Journal of Materials Research and Technology, 20, 3714-3722.
5. Yuan, J. J., Kong, Q. R., Huang, Z., Song, Y. Z., Li, M. Y., Fang, L. F., ... & Li, H. Y. (2021). A well-designed polymer as a three-in-one multifunctional binder for high-performance lithium–sulfur batteries. Journal of Materials Chemistry A, 9(5), 2970-2979.
6. He, M., Yuan, L. X., Zhang, W. X., Hu, X. L., & Huang, Y. H. (2011). Enhanced cyclability for sulfur cathode achieved by a water-soluble binder. The Journal of Physical Chemistry C, 115(31), 15703-15709.
7. Lee, J., Heo, K., Song, Y. W., Hwang, D., Kim, M. Y., Jeong, H., ... & Lim, J. (2021). Degradation of all-solid-state lithium-sulfur batteries with PEO-based composite electrolyte. Journal of Electrochemical Science and Technology, 13(2), 199-207.
8. Kuz'mina, E. V., Karaseva, E. V., Chudova, N. V., Mel'nikova, A. A., & Kolosnitsyn, V. S. (2019). On the possibility of determination of thermodynamic functions of the Li–S electrochemical system using the EMF method. Russian Journal of Electrochemistry, 55, 978-988.
9. Barchasz, C., Leprêtre, J. C., Alloin, F., & Patoux, S. (2012). New insights into the limiting parameters of the Li/S rechargeable cell. Journal of Power Sources, 199, 322-330.
10. Nakamura, N., Ahn, S., Momma, T., & Osaka, T. (2023). Future potential for lithium-sulfur batteries. Journal of Power Sources, 558, 232566.
11. Zhang, B., Qin, X., Li, G. R., & Gao, X. P. (2010). Enhancement of long stability of sulfur cathode by encapsulating sulfur into micropores of carbon spheres. Energy & Environmental Science, 3(10), 1531-1537.
12. Dai, W., Ma, Z., Wang, D., Yang, S., & Fu, Z. (2022). Functional multilayer solid electrolyte films for lithium dendrite suppression. Applied Physics Letters, 121(22), 223901.
13. Li, J., Yuan, C. F., Guo, Z. H., Zhang, Z. A., Lai, Y. Q., & Liu, J. (2012). Limiting factors for low-temperature performance of electrolytes in LiFePO4/Li and graphite/Li half cells. Electrochimica acta, 59, 69-74.
14. Sun, Y., Zhang, Y., Xu, Z., Gou, W., Han, X., Liu, M., & Li, C. M. (2022). Dilute Hybrid Electrolyte for Low-Temperature Aqueous Sodium-Ion Batteries. ChemSusChem, e202201362.
15. Deng, Z., Zhang, Z., Lai, Y., Liu, J., Li, J., & Liu, Y. (2013). Electrochemical impedance spectroscopy study of a lithium/sulfur battery: modeling and analysis of capacity fading. Journal of The Electrochemical Society, 160(4), A553.
16. Zhou, W., Yu, C., & Wang, X. (2022). Fast and Quantitative Electrical Detection of Iodine Based on a Polymer of Intrinsic Microporosity. ACS Applied Polymer Materials, 4(12), 9151-9159.
17. Holzapfel, M., Martinent, A., Alloin, F., Le Gorrec, B., Yazami, R., & Montella, C. (2003). First lithiation and charge/discharge cycles of graphite materials, investigated by electrochemical impedance spectroscopy. Journal of Electroanalytical Chemistry, 546, 41-50.
18. Lieu, W. Y., Fang, D., Li, Y., Li, X. L., Lin, C., Thakur, A., ... & Seh, Z. W. (2022). Spherical Templating of CoSe2 Nanoparticle-Decorated MXenes for Lithium–Sulfur Batteries. Nano Letters, 22(21), 8679-8687.
19. Chen, H., Hong, H., Zhang, X., Zhang, Y., Liu, J., & Zheng, Y. (2022). Integration of porous graphitic carbon and carbon fiber framework for ultrahigh sulfur-loading lithium–sulfur battery. Dalton Transactions, 51(8), 3357-3365.
20. Yu, C. W., & Tsai, C. J. (2022). Ti4O7 as conductive additive in sulfur and graphene-sulfur cathodes for high-performance Lithium-sulfur batteries with a facile preparation method. MRS Energy & Sustainability, 9(2), 369-377.
21. Gerle, M., Wagner, N., Häcker, J., Nojabaee, M., & Friedrich, K. A. (2022). Identification of the Underlying Processes in Impedance Response of Sulfur/Carbon Composite Cathodes at Different SOC. Journal of The Electrochemical Society, 169(3), 030505.
22. Elazari, R., Salitra, G., Talyosef, Y., Grinblat, J., Scordilis-Kelley, C., Xiao, A., ... & Aurbach, D. (2010). Morphological and structural studies of composite sulfur electrodes upon cycling by HRTEM, AFM and Raman spectroscopy. Journal of The Electrochemical Society, 157(10), A1131.